Experimental study of the frequency repulsion effect

(Submitted to Am. J. Phys. March 2007)

R. F. Gamarra[1], M. Josebachuili[1], P. Zurita[1] and S. Gil[1,2,a]

[1] Departamento de Física, "J. J. Giambiagi," F.C.E.y N., Universidad de Buenos Aires, Argentina
[2] Escuela de Ciencia y Tecnología, Universidad Nacional de San Martín, Campus Miguelete, M. de Irigoyen 3100, San Martín (1650), Buenos Aires, Argentina

01.50.Pa, 03.65.Sq,07.05.Hd,07.50.Ek,07.50.Qx,31.15.Md

In this work we present an experiment to study the resonance curves of coupled RLC circuits with variable coupling strength. The inductive coupling can be easily varied and measured for the different configurations. Our setup allows us to explore thoroughly the variation of the resonance frequencies as a function of the coupling strength between the oscillators. This system can be used to illustrate the effect of eigenfrequency repulsion when an interaction couples different modes of oscillation. This effect is prevalent in many classical and quantum mechanical systems. The experiment is conceptually simple and its results can be quantitatively compared with the theoretical predictions.

I. Introduction

The study of coupled oscillators is of interest in several areas of physics and engineering. An interesting and important phenomenon present in these systems is the frequency repulsion effect. A system of two coupled oscillators has two eigenfrequencies.[1] A remarkable phenomenon takes place as one varies the interaction between them. As the coupling strength increases, the lower eigenfrequency decreases while the higher increases, i.e. there is a "repulsion" between the eigenfrequencies. This effect has a quantum mechanical analog (level repulsion) known as the Wigner-von Neumann anti-crossing rule,[2] that has very important consequences in molecular, atomic, nuclear and particle physics.[3,4,5] An interesting example is the case of the ammonia molecule in an electric field.[3] Other examples include the hyperfine splitting of the hydrogen atom in a magnetic field,[3] the Nilsson model for deformed nuclei[6,7] and the neutrino oscillation between flavors.[8] However, there are few experiments that illustrate the consequences of this important effect in the literature.[9,10] Thus, it is useful to develop experiments that illustrate this phenomenon. The example we will discuss here is an inductively coupled RLC circuit. This system is conceptually simple to understand by beginner and intermediate students and the experiment is low cost and readily accessible. Moreover, the coupling strength can be easily measured and modified in a continuous and convenient way. In this manner, the basic characteristic of the eigenfrequency repulsion effect is clearly illustrated. Furthermore, it is possible to develop a simple theoretical model that accounts for the experimentally observed data quite well. It is also accessible to students with a basic background in circuit theory. Preceding qualitative studies[9] performed with different experimental set-ups and techniques lacked the necessary sensitivity and accuracy, but paved the way for the present approach.

There are several ways to perform this experiment. Here we employ a Lock-In Amplifier.[11] The motivation for using this device is that Lock-In Amplifiers (LIA) are very versatile and useful instruments, increasingly used in most research and industrial settings. LIA are particularly useful when we are interested in detecting small signals of known frequencies in the presence of a noisy environment. Furthermore, there have been several developments that have made the LIA available to teaching laboratories with modest budgets.[12,13] Also a LIA can be used to obtain the frequency response or the frequency spectrum of a system in a very convenient and practical manner. Although the LIA is a useful tool for carrying out this experiment, it is not essential and a good oscilloscope could be used instead, at the expense of making the experiment more time consuming and far less sensitive to small signals.

II. Theoretical considerations

The theory of the frequency repulsion effect has been discussed extensively in the literature.[3,4,5] The basic aspect of the physical process involved in the frequency repulsion can be illustrated in the case of a coupled harmonic oscillator. Therefore we briefly review the case of two inductively coupled LC circuits as indicated schematically in Fig. 1.

Applying Kirchhoff's law to the circuit of Fig. 1 we have:

$$\frac{q_1}{C_1} + L_1 \cdot \frac{di_1}{dt} \pm M \cdot \frac{di_2}{dt} = 0 \tag{1}$$

and

$$\frac{q_2}{C_2} + L_2 \cdot \frac{di_2}{dt} \pm M \cdot \frac{di_1}{dt} = 0\,. \tag{2}$$

Here $q_k(t)$ and $i_k(t)=dq_k(t)/dt$ are the charges and the currents in the circuits 1 (left) and 2 (right). M is the mutual inductance coefficient that depends on the distance between the coils and their geometric configuration. The different signs for M are related to the relative orientation of the induction coils[14] L_1 and L_2. Furthermore, the condition $M^2 \leq L_1 \,.\, L_2$ must be satisfied.[14] To solve this system of coupled differential equations we assume that:

$$q_k(t) = A_k \cdot Exp(j\omega \cdot t)\,, \tag{3}$$

replacing Eq. (3) into Eqs. (1) and (2) yields:

$$\frac{A_1}{C_1} - L_1 \cdot A_1 \cdot \omega^2 \mp M \cdot A_2 \cdot \omega^2 = 0 \tag{4}$$

and

$$\frac{A_2}{C_2} - L_2 \cdot A_2 \cdot \omega^2 \mp M \cdot A_1 \cdot \omega^2 = 0\,. \tag{5}$$

Defining:

$$\omega_{10}^2 = \frac{1}{L_1 \cdot C_1} \quad \text{y} \quad \omega_{20}^2 = \frac{1}{L_2 \cdot C_2}\,, \tag{6}$$

it is possible to cast the Eqs.(4) and (5) in the following matrix form:

$$\begin{pmatrix} (\omega_{10}^2-\omega^2) & \mp\dfrac{M}{L_1}\cdot\omega^2 \\ \mp\dfrac{M}{L_2}\cdot\omega^2 & (\omega_{20}^2-\omega^2) \end{pmatrix}\cdot\begin{pmatrix} A_1 \\ A_2 \end{pmatrix}=0\,. \tag{7}$$

There is a solution for this system of equations, different from the trivial (A_1=A_2=0), only if the determinant of this matrix is null, i.e.:

$$\begin{vmatrix} (\omega_{10}^2-\omega^2) & \mp\dfrac{M}{L_1}\cdot\omega^2 \\ \mp\dfrac{M}{L_2}\cdot\omega^2 & (\omega_{20}^2-\omega^2) \end{vmatrix}=(\omega_{10}^2-\omega^2)\cdot(\omega_{20}^2-\omega^2)-\frac{M^2}{L_1\cdot L_2}\cdot\omega^4=0 \tag{8}$$

If we define:

$$\alpha=\frac{M^2}{L_1\cdot L_2} \qquad \text{with} \qquad 0\le\alpha\le 1\,, \tag{9}$$

the eigenfrequencies of the coupled system are:

$$\widetilde{\omega}^2=\frac{1}{2(1-\alpha)}\left[(\omega_{10}^2+\omega_{20}^2)\pm\sqrt{\omega_{10}^4+\omega_{20}^4-2(1-2\alpha)\cdot\omega_{10}^2\cdot\omega_{20}^2}\right]. \tag{10}$$

From this expression it follows that:

$$\left|\widetilde{\omega}_1^2-\widetilde{\omega}_2^2\right|\ge\left|\omega_{10}^2-\omega_{20}^2\right|. \tag{11}$$

This relation implies that the difference between eigenfrequencies in the coupled system is always larger than that of the uncoupled case. Furthermore, the ratio $\left|\widetilde{\omega}_1^2-\widetilde{\omega}_2^2\right|\div\left|\omega_{10}^2-\omega_{20}^2\right|$ increases monotonically with α and independently of the sign of coupling strength (M). This is basically the content of the frequency repulsion effect, which prevails in both coupled classical and quantum systems.

The quantum analog of this phenomenon is the level repulsion effect, which has also been discussed in the literature.[3,4,5] A simple justification of this effect can be given by considering a two level system. Assume that in the absence of interaction we have a Hamiltonian H_0 with eigenenergies E_1^0 and E_2^0 i.e.

$$H_0\psi_i^0=E_i^0\psi_i^0\,, \qquad \text{with} \quad i=1,2. \tag{12}$$

where ψ_i^0 are the eigenfunctions of the Hamiltonian H_0 corresponding to the eigenvalues E_i^0. If an interaction V is introduced, that mixes the states 1 and 2, with the properties:

$$\left\langle\psi_j^0\middle|V\middle|\psi_i^0\right\rangle=V_0(1-\delta_{j,i})\,. \tag{13}$$

Then the new (perturbed) Hamiltonian H=H_0+V has eigenenergies E_i given by:[3,4,5]

$$E_{1,2}=\frac{1}{2}\left[\left(E_1^0+E_2^0\right)\pm\sqrt{(E_2^0-E_1^0)^2+4V_0^2}\right]. \tag{14}$$

Therefore, the energy difference has the following property:

$$\left|E_2-E_1\right|=\sqrt{(E_2^0-E_1^0)^2+4V_0^2}\ge\left|E_2^0-E_1^0\right|. \tag{15}$$

Eq. (15) indicates that the energy difference increases monotonically with the magnitude of the coupling strength V_0, independently of its sign. [3,4,5]

III. The Experiment

To experimentally study the frequency repulsion effect we built a coupled classical RLC resonator illustrated in Figs. 2 and 3. Here x is the axial distance between the two coils with x=0 corresponding to the case when the two coils are side by side. Fig. 3 is the physical realization of the circuit shown in Fig. 2. The presence of the resistances in the circuits has a double origin. Inductances always have some internal resistance and the external resistances ($\widetilde{R}_i$) are useful for monitoring the responses (currents) of the circuits. In a single RLC (series) the resonance frequency coincide with the natural fequency.[14] Therefore, to characterize the natural frequencies of a coupled RLC circuit we built an experimental setup that allow us to study the resonance curve in this circuit. The two coupled RLC circuits have parameters indicated in Table 1. The internal resistance of the AC source (function generator) is r. r_{L1} and r_{L2} are the internal resistances of inductances L_1 and L_2 respectively. We denote with $\widetilde{R}_1$ and $\widetilde{R}_2$ the external resistors in the primary and secondary circuits respectively, whereas R_1 and R_2 denote the total resistance in these circuits. The voltage drops across the external resistances (V_{R1} and V_{R2}) are used alternatively as input for the LIA. The currents in the primary and secondary circuit are obtained by the ratios $V_{R1}/\widetilde{R}_1$ and $V_{R2}/\widetilde{R}_2$ respectively. The internal oscillator of the LIA is used to power the primary loop. The value of all the parameters of our circuit can be known and were measured independently, including the internal resistance of the coils and the internal resistance of the AC power supply. The coils were made of copper wires gauge #26 (diameter=0.4 mm) of 1040 turns. These coils had an internal diameter of 2.5 cm, an external diameter of 5.2 cm and a width of 2 cm. The two coils could snuggly move over a common wooden rod. This arrangement allowed for a very convenient way of varying the distance between the coils and consequently the mutual induction M of the system (coupling strength).

The value of M as a function of the distance between the two coils (x) was determined in an independent manner. For this purpose we simply measured the induced voltage in the secondary inductance (L_2) alone with no other component connected. From definition[14] of M we have:

$$\varepsilon_2 = -M\frac{di_1}{dt}. \tag{16}$$

Since we excited the circuit with a sinusoidal signal of frequency f_0, from the linearity of the system it follows that the amplitude of the induced emf, ε_2^0, is given by:

$$\varepsilon_2^0 = -M\cdot 2\pi f_0 \frac{V_{R1}^0}{\widetilde{R}_1}. \tag{17}$$

This expression allows us to obtain M for each configuration from the measurements of the amplitude of the voltage drop across $\widetilde{R}_1$ (V_{R1}^0) and the amplitude of the induced emf in the secondary inductance. This procedure was used to study how M varies with x, to determine how the coupling factor changes for the different geometrical configurations. Once we obtained M for different values of x, we measured the voltages drops on both $\tilde{R}_1$ and $\tilde{R}_2$ in

the same geometrical configurations we used for M, i.e. V_{R1}^0 and V_{R2}^0 as a function of the frequency.

To characterize the frequency response of our coupled oscillator, we used a digital lock-in amplifier SR830, controlled by a computer. This arrangement allowed us to measure the magnitude of the current for each excitation frequency. The computer allowed us to sweep the excitation frequency between 1 kHz to 40 kHz, at a preset step, 500 Hz. As indicated in Fig.3, the reference output of the LIA was used to feed the circuit (ac source). Further technical details on this experiment can be found in Internet[15].

IV. Results and Discussion

In Fig. 4 we show, in a semilog plot, both the variation of M as a function of x and an empirical fit to the data. The diamonds represent the values obtained by the measurement of the emf in the secondary selfinductance as described above. Thus this figure provides the value of M for any value of x.

Fig. 5 shows the results of the response of the primary circuit, i.e. the amplitude of the current in the primary circuit ($V_{R1}/\tilde{R}_1$), for different separations of the coils. For a large separation of the coils (uncoupled system) we observe the response of the primary circuit alone. Adjusting the parameters of the theoretical model to the experimental results it is possible to obtain the parameters (L_1, C_1, etc) of the system. In Table 1 the values thus obtained are compared to those obtained by direct measurements of the individual components. The values agree within a few percent, indicating the consistency of the methods employed.

In Fig. 6 we show the response of the secondary circuit (using V_{R2} as input for the LIA) for different separations. In this figure we also include the response of the secondary circuit when the system is uncoupled. To obtain the resonance curve for this case we simply excited the secondary circuit (alone) with the reference output of the LIA. The widening in the uncoupled curve is due to the presence of the internal resistance of the function generator ($r \approx 50\ \Omega$) used to excite the secondary circuit. Note that as the coupling decreases (x increases) the amplitude of the signal in the secondary also diminishes. The larger signal observed in the uncoupled case is consequence of the direct mode we used to excite this system. Despite these differences, the frequencies of the maxima in the uncoupled and weakest coupling cases coincide as expected.

Figs. 5 and 6 clearly show that when there is coupling between the two systems, there is a bimodal resonance curve. Furthermore, the positions of its maxima tend to separate for smaller distances between the coils (larger coupling strength between them) in consonance with the theoretical expectation, Eq. (10).

In Fig. 7 we present the results of the current amplitude for the primary and secondary circuits for x=0. The symbols indicate the results of the measured current amplitude, in primary and secondary circuits, see Fig. 2. In this figure we have also plotted the corresponding theoretical prediction obtained using expressions (A10) and (A11). This figure illustrates how well the theory reproduces the experimental data. The adjustable

parameters of the model are the values of M, R_i, L_i and C_i. The values of these parameters obtained from this fit are indicated in the third column of Table 1. Therefore, this procedure (fitting the model to the data) provides another way of measuring M as well as the rest of the parameters. As Table 1 indicates, the results of these parameters thus obtained, agree very well with those obtained using direct measurements.

Fig. 8 illustrates the effect of "level repulsion". Here we plotted with square symbols and triangles the eigenfrequencies (position of the maxima of the secondary circuit of Fig. 6) as a function of the distance between the coils. As indicated in Fig. 4, this distance is associated with the coupling strength. Fig. 8 clearly shows that as the distance decreases (coupling strength increases) the repulsion effect is enhanced (i.e. the difference between the eigenfrequencies increases), in agreement with expression (10). For large separations between the coils the eigenfrequencies, as expected, converge to the uncoupled values. In addition to the experimental data, the theoretical expectations, Eq.(10), are indicated by the heavy lines.

V. Conclusions

Our experimental setup is a very simple and useful device for studying the basic characteristics of a coupled oscillator with variable coupling strength. The effect of eigenfrequencies repulsion is readily observable, which is an important phenomenon prevalent in both classical and quantum systems. The theoretical model developed to account for the experimental results provides an excellent description of the data. The experiment and the theoretical model can be generalized to the case of several coupled oscillators. Finally, this experiment provides an instructive and useful application of the Lock-In amplifier for studying interesting and instructive phenomena.

We would like to express our acknowledgement to other students that have explored the physics of our systems with different experimental techniques.

We also express our gratitude to Prof. Carlos Acha for his assistance in the setting and programming of the LIA and to the valuable comments and suggestions made by Dr. E. Batista and Prof. C. Grosse. We are also grateful to Dr. A. Schwint a careful reading of the manuscript.

[a]) Electronic mail: **sgil@unsam.edu.ar**

Appendix A

Forced coupled RLC circuits

Consider the circuit illustrated in Fig. 2. An AC source powers the left network (primary). We characterize the voltage generated by the AC power source as: $v_1(t)=V_{10}.exp(-j\omega t-\phi)$, where V_{10} is the amplitude of the signal, ω the angular frequency, j the imaginary unit and ϕ the phase difference with the current in the primary. Measuring the voltage drop across the resistances $\widetilde{R}_1$ and $\widetilde{R}_2$ the current in each loop can be monitored. In the following analysis R_1 and R_2 are the total resistance of the primary and secondary loops. They include the internal

resistance of the source (primary) and the ohmic resistance of the inductances. To solve this circuit we assume that:[14,16]

$$i_1(t) = I_{10}\exp(j\omega t) \quad \text{and} \quad i_2(t) = I_{20}\exp(j\omega t + \varphi_2). \tag{A1}$$

The complex impedance[14,16] of the left and right loop are respectively:

$$Z_1(\omega) = R_1 + j(L_1 \cdot \omega - 1/\omega C_1) = R_1 + jX_1(\omega) \tag{A2}$$

and

$$Z_2(\omega) = R_2 + j(L_2 \cdot \omega - 1/\omega C_2) = R_2 + jX_2(\omega) \tag{A3}$$

According to Kirchhoff's laws we have:

$$V_{10}\exp(j\omega t - \phi) = Z_1(\omega)\cdot i_1(t) - M \cdot j\omega \cdot i_2(t) \tag{A4}$$

and

$$Z_2(\omega)\cdot i_2(t) - M \cdot j\omega \cdot i_1(t) = 0\,. \tag{A5}$$

Solving for $i_2(t)$ yields:

$$V_{10}\exp(j\omega t - \phi) = i_1(t)\cdot\left(Z_1(\omega) + \omega^2 M^2/Z_2(\omega)\right) = i_1(t)\cdot Z_1'(\omega) \tag{A6}$$

with

$$Z_1'(\omega) = \left(R_1 + \frac{\omega^2 M^2 R_2}{R_2^2 + X_2^2}\right) + j\left(X_1 - \frac{\omega^2 M^2 X_2}{R_2^2 + X_2^2}\right) = R_e + jX_e(\omega)\,. \tag{A7}$$

The solutions for i_1 and i_2 are:

$$i_1(t) = I_{10}\exp(j\omega t) = V_{10}\exp(j\omega t - \phi)\cdot\left(Z_2(\omega)/\left(Z_1(\omega)\cdot Z_2(\omega) + \omega^2 M^2\right)\right) \tag{A8}$$

and

$$i_2(t) = I_{20}\exp(j\omega t + \varphi_2) = j\cdot V_{10}\exp(j\omega t - \phi)\cdot\left(M\omega/\left(Z_1(\omega)\cdot Z_2(\omega) + \omega^2 M^2\right)\right). \tag{A9}$$

The magnitude of the current amplitudes, I_{10} and I_{20}, can be written as:

$$I_{10} = V_{10}\cdot\left(\frac{\sqrt{R_2^2 + X_2^2}}{D}\right) \quad \text{y} \quad I_{20} = V_{10}\cdot\left(\frac{\omega \cdot M}{D}\right) \tag{A10}$$

with

$$D^2 = \left[\left(R_1R_2 - X_1X_2 + \omega^2M^2\right)^2 + \left(R_1X_1 + R_2X_1\right)^2\right]. \tag{A11}$$

The expressions (A19) and (A11) are the stationary solution of the coupled circuit. These expressions can be directly compared with the results of our measurements. The continuous lines in Figs. 6 and 10 were obtained using Eqs. (A10) and (A11).

Figure captions

Fig. 1. Inductively coupled LC circuits.

Fig. 2. Inductively coupled RLC circuits. The resistance r is the internal resistance of the AC source and r_{L1} and r_{L2} are the internal resistances of the inductances L_1 and L_2 respectively. The voltage drop in the resistances of the primary and secondary circuits are measured directly by the Lock-In amplifier. V_{Ri} is the voltage drop in the resistance $\widetilde{R}_i$ and is used to monitor the currents in each network.

Fig. 3. Schematic diagram of the experimental setup. The two coils move along a wooden rod. Here x is the separation between the coils. An AC source is connected to the primary circuit.

Fig. 4. Experimental results of the mutual inductance M as a function of the separation distance x. The diamond symbols are the results of M obtained by direct measurement of this value. The continuous line is an empirical fit to the data using an exponential function.

Fig. 5. Experimental result of the amplitude in the primary circuit, for different separations between the coils. The position of the maxima of these curves tend to separate for small distances, i.e. stronger coupling.

Fig. 6. Experimental result of the amplitude of the secondary circuit current for different separations between the coils. Note that the maxima of these curves tend to separate for small distances, i.e. stronger coupling.

Fig. 7. Experimental results of the current amplitude in the primary (crosses) and secondary (circles) circuits for x=0. The continuous lines are fits to the data using the theoretical Eq. (A10) with the mutual induction coefficient $M(x)$ as the only adjustable parameter. The results of M thus obtained for each value of the separation distance x are shown in Fig. 4.

Fig. 8. Experimental result of the resonance maxima as a function of the separation distance x. The heavy lines are the result of our model Eq. (10). The dotted horizontal lines indicate the uncoupled eigenfrequencies.

Table

	Direct measurement	From best fit of the model
$\widetilde{R}_1$	15 ± 1 Ω	
$\widetilde{R}_2$	7 ± 1 Ω	
r	50 ± 2 Ω	
r_{L1}	18 ± 1 Ω	
r_{L2}	19 ± 1 Ω	
R_1	83± 3 Ω	90 ± 4 Ω
R_2	26 ± 3 Ω	31 ± 4 Ω
L_1	32.4 ± 0.2 mHy	32 ± 5 mHy
L_2	33.5 ± 0.2 mHy	34 ± 5 mHy
C_1	99.1 ± 0.2 nF	99 ± 7 nF
C_2	108 ± 0.2 nF	108 ± 3 nF

Table 1. Values of the parameters used in the system. The second column shows the values of the parameters obtained by direct measurements. The third column shows the results obtained from fit of the data, as illustrated in Fig. 6. In this case the model only provides the total resistance of the circuit.

References

[1] H. Goldstein, C. Poole, and J. Safko, Classical Mechanics (Addison-Wesley, Boston, MA, 2001), 3rd ed.

[2] J. von Neumann and E. Wigner, "ÄUber das Verhalten von Eigenwerten bei adiabatischen Prozessen, " Z. Phys., **30,** 467-470 (1929).

[3] R.P. Feynman, R.B. Leighton, and M.Sand, *Feynman Lectures On Physics*, (Addison-Wesley, Reading, MA, 1970), Vol. 3, Chaps. 9-11.

[4] C. Cohen-Tannoudji, B. Diu, and F. Laloe, *Quantum Mechanics* (Wiley, N.Y. 1977) Vol.1, Chap.4.

[5] W. Frank and P. von Brentano, "Classical analogy to quantum mechanical level repulsion," Am. J. Phys. **62**, 706-709 (1994)

[6] P. Ring and P. Schuck, *The nuclear many-body problem*, (Springer-Verlag, N.Y. 1980)

[7] Introduction to Nuclear Properties from the department of physics, University of Jyväskylä, Finland, http://www.phys.jyu.fi/research/gamma/publications/ptgthesis/node7.html

[8] E. Sassaroli, 'Neutrino oscillations: A relativistic example of a two-level system,' Am. J. Phys. **67**, 869–875 (1999).

[9] H.A. Atwater, "Laboratory exercises in Classical Electromagnetic Field Theory," Am. J. Phys. **36**, 672-682 (1968)

[10] C.L. Garrido Alzar , M.A.G. Martinez and P. Nussenzveig, "Classical analogy of electromagnetically induced transparency," Am. J. Phys. **70**,37-41 (2002)

[11] J.H. Scofield, "Frequency-domain description of a lock-in amplifier," Am. J. Phys. **62** 129 (1994).

[12] S. K. Sengupta, J. M. Farnham, and J. E. Whitten, "A Simple Low-Cost Lock-In Amplifier for the Laboratory," J. of Chem. Educ. **82** (9) 1400-1401 (2005)

[13] National Instruments, "Creating a Lock-In Amplifier with LabVIEW", http://zone.ni.com/devzone/cda/tut/p/id/4026

[14] J. R. Reitz, J. R. Milford, and R. W. Christy, *Foundations of Electromagnetic Theory*, (4th ed. Addison-Wesley, Reading, MA, 1993).

[15] Further technical details on our experiment and copy of the Excel file used to fit the experimental results (Figs. 5 and 6), can be downloaded from www.fisicarecreativa.com. This site also describes experimental projects and reports of experiments performed by undergraduate students from several Latin American universities.

[16] B. Kurrelmeyer and W.H. Mais, *Electricity and Magnetism,* (Van Nostrand, Princeton, N.J. 1967)

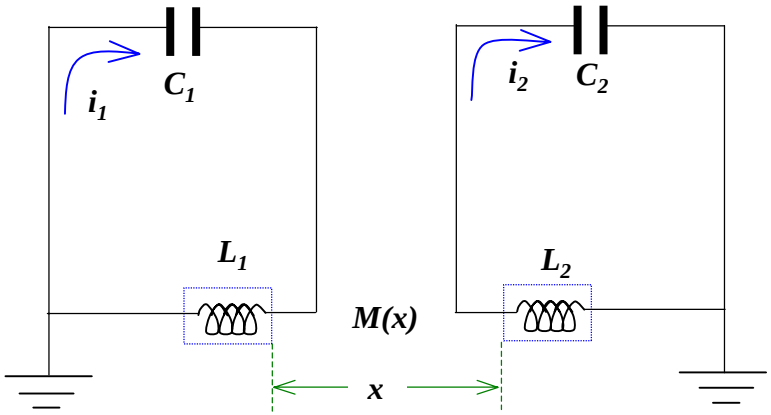

Fig. 1

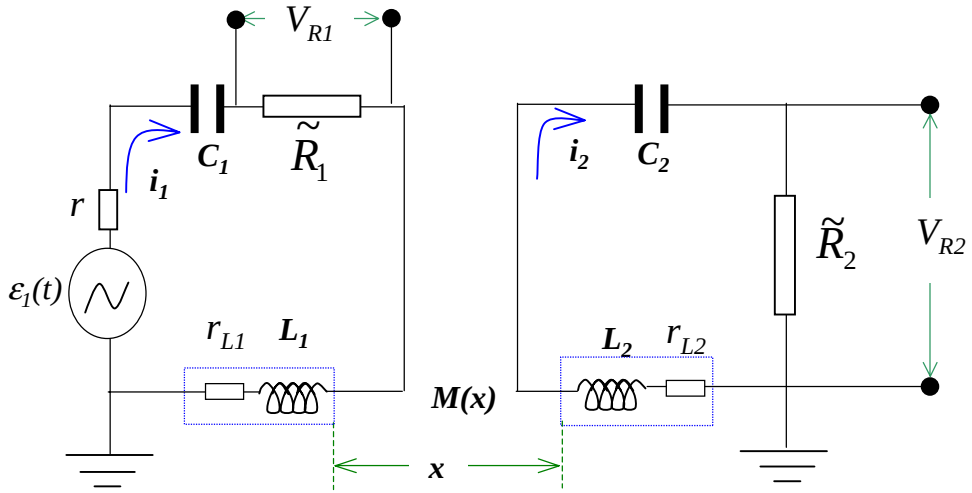
V_{R1}
C_1
$\tilde{R}_1$
i_1
r
$\varepsilon_1(t)$
r_{L1}
L_1
$M(x)$
x
i_2
C_2
$\tilde{R}_2$
V_{R2}
L_2
r_{L2}

Fig. 2

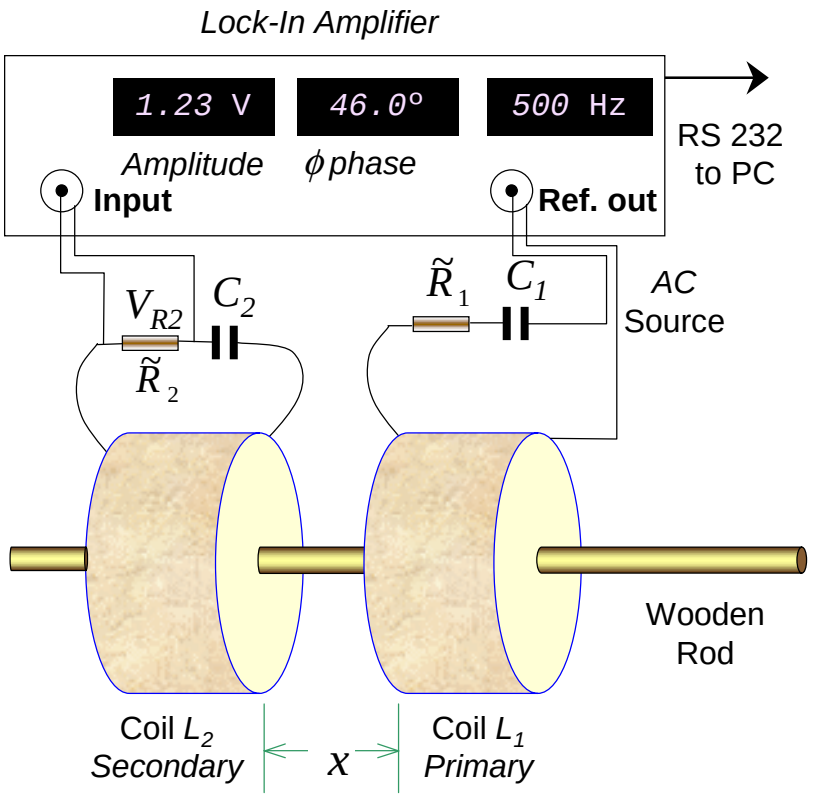
Lock-In Amplifier
1.23 V
46.0°
500 Hz
Amplitude
ϕ phase
RS 232
to PC
Input
Ref. out
V_{R2}
C_2
$\tilde{R}_2$
$\tilde{R}_1$
C_1
AC
Source
Wooden
Rod
Coil L_2
Secondary
x
Coil L_1
Primary

Fig. 3

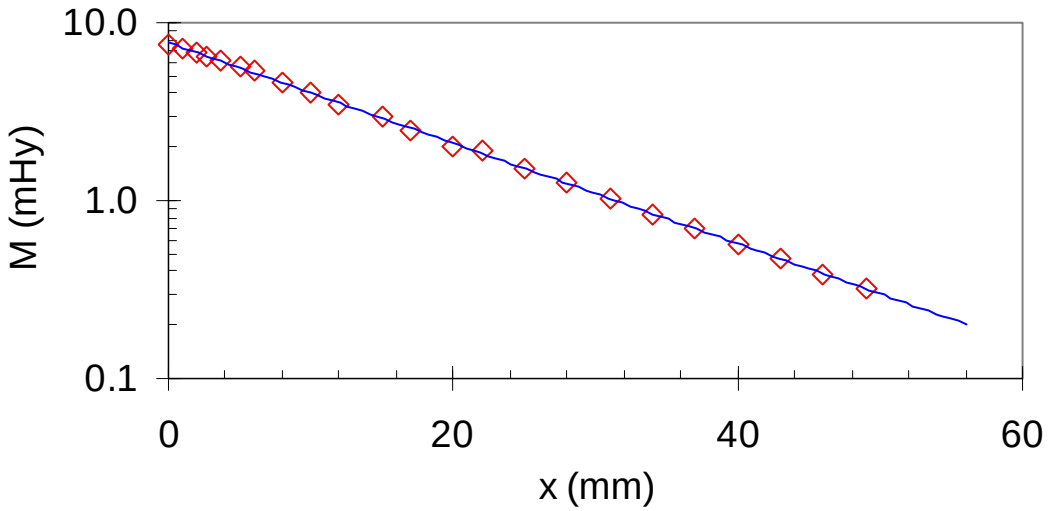

Fig. 4

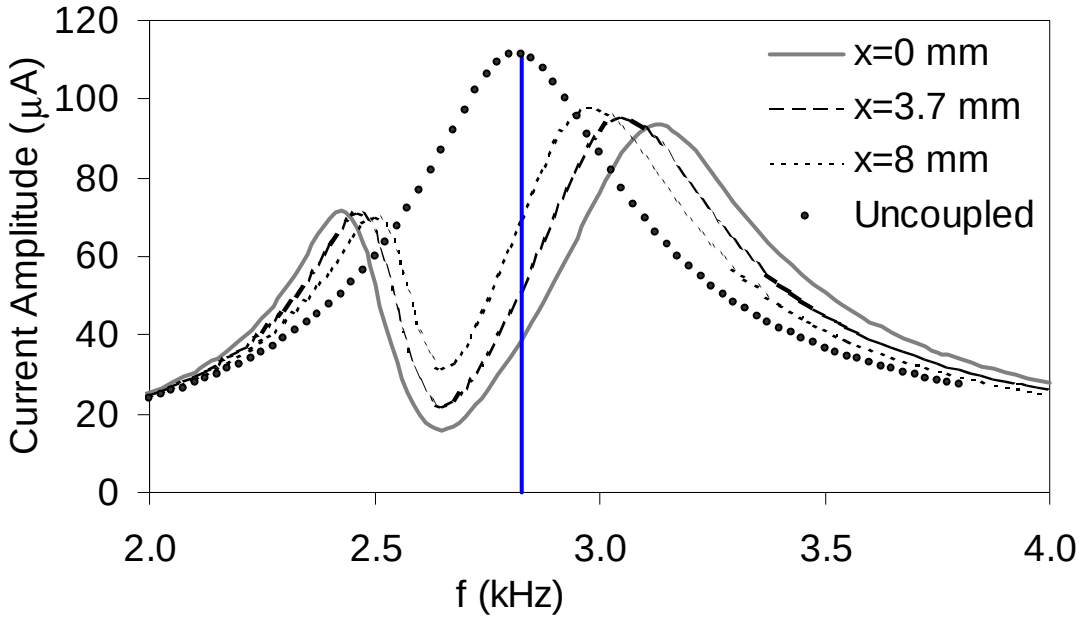
120
100
80
60
40
20
0
Current Amplitude (μA)
2.0
2.5
3.0
3.5
4.0
f (kHz)
x=0 mm
x=3.7 mm
x=8 mm
Uncoupled

Fig. 5

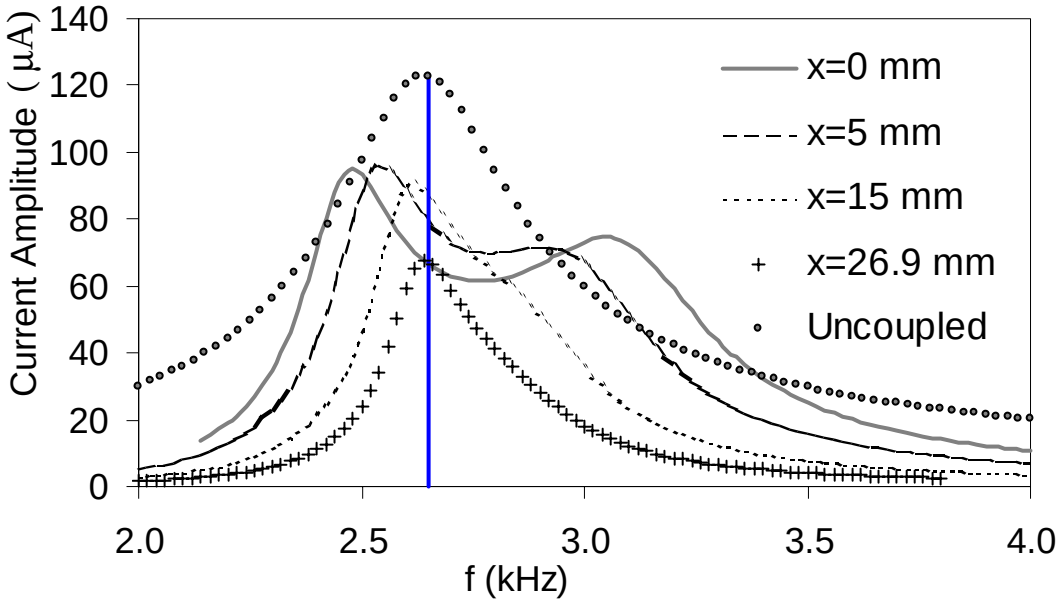
Current Amplitude (μA)
140
120
100
80
60
40
20
0
2.0
2.5
3.0
3.5
4.0
f (kHz)
x=0 mm
x=5 mm
x=15 mm
x=26.9 mm
Uncoupled

Fig. 6

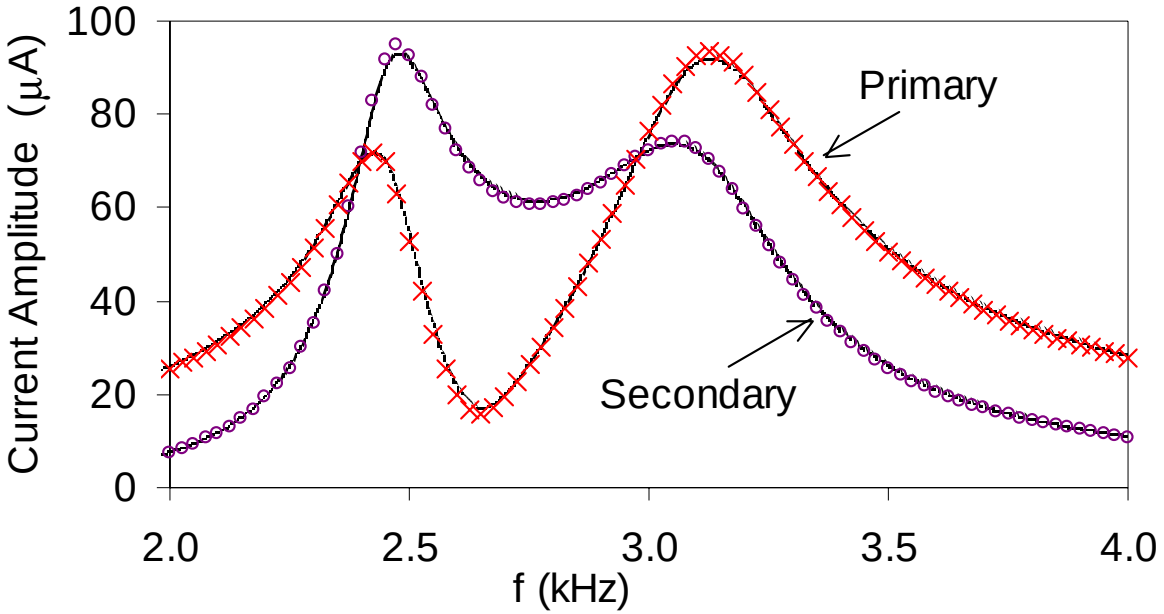
Current Amplitude (μA)
100
80
60
40
20
0
2.0
2.5
3.0
3.5
4.0
f (kHz)
Primary
Secondary

Fig. 7

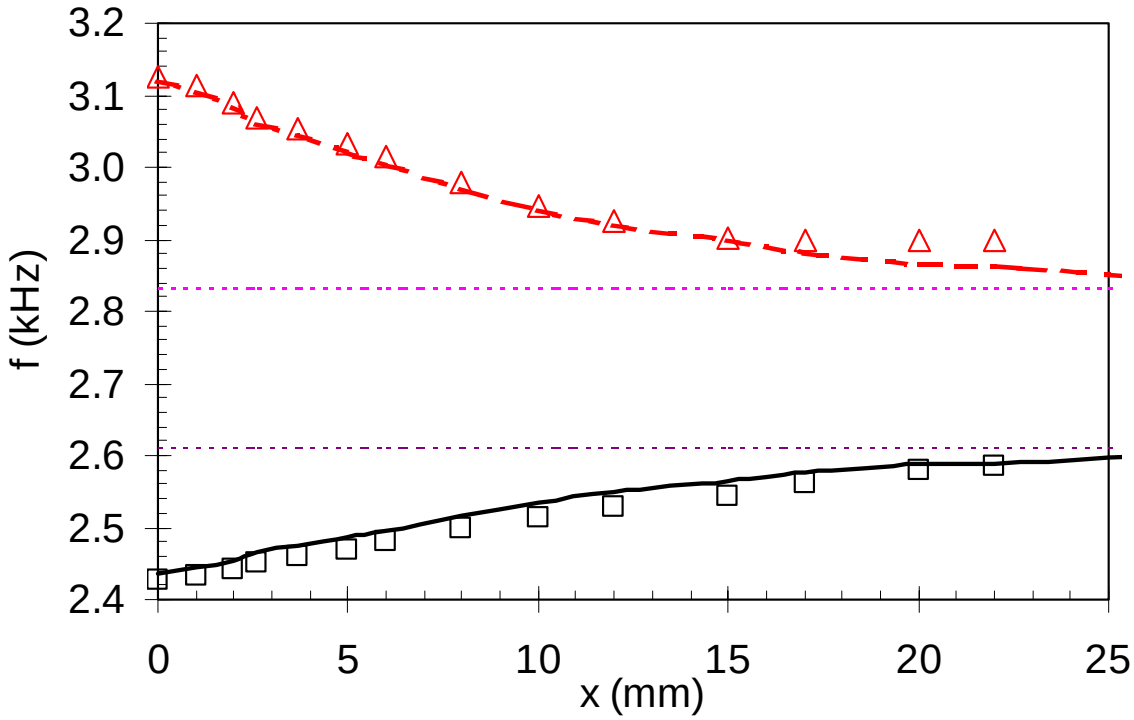

Fig. 8